Repeated binge drinking causes plastic increases in central amygdala corticotropin releasing factor neurons *in vivo*

James M Irving[1]*, Sonia Aroni[1]*, Kasey S. Girven[1,2], Dennis R Sparta[1,2]

[1]Department of Anatomy and Neurobiology, University of Maryland School of Medicine, Baltimore MD 21201, USA
[2]Program in Neuroscience, University of Maryland Baltimore, Baltimore, MD 21201, USA

Abbreviated title: Ethanol increases CeA CRF neurons

*These authors contributed equally to this work

Corresponding Author:
Dennis R. Sparta, Ph.D.
University of Maryland School of Medicine
Department of Anatomy and Neurobiology
20 Penn St, Rm 280K
Baltimore MD, 21201
Tel 410-706-3814
Email: dsparta@som.umaryland.edu

Number of Figures: 4

Number of Words for Abstract: 222

Abstract

Binge ethanol drinking is an increasingly problematic component of alcohol use disorder costing the United States approximately over $150 billion every year. Binge drinking likely causes progressive neuroplasticity alterations in numerous brain regions. However, the precise nature or mechanisms by which they alter binge drinking have not yet been determined. Corticotropin releasing factor (CRF) neurons in the central amygdala (CeA) are thought to modulate binge drinking, but the precise circuit mechanisms remain poorly understood. Here, for the first time we combined optogenetics with *in vivo* electrophysiology to identify and record from CeA CRF neurons in mice during a repeated binge drinking task. First, we found that CeA CRF neurons were more excitable than CeA non CRF neurons in our binge drinking. We also observed that CeA CRF neurons displayed a heterogeneous spike profile in response to a lick of ethanol including lick predictive, lick excited, lick inhibited, and no response. Lick predictive CeA CRF neurons could be further grouped into 2 classes based on their activity in response to a binge alcohol session, with the majority showing increases in firing and bursting. Furthermore, lick predictive CeA CRF neurons increased their activity over repeated binge drinking sessions, indicating possible synaptic plasticity. These data indicate that microcircuits within the CeA CRF system as well as their projections may modulate specific components of binge drinking.

Introduction

Alcohol use disorder (AUD) is a progressive and persistent disease characterized by frequent cycles of binge/intoxication, withdrawal and craving. Alcohol related health costs in the United States costs over 200 billion dollars annually. In particular, binge drinking accounts for 75% of the societal cost attributed to AUD[1]. Moreover, it is linked to the progressive dysfunction of multiple organs and is considered a first step in the development of AUD[2]. Behavioral consequences of binge drinking are mediated by long-term alterations in brain stress circuits residing within the extended amygdala[3]. However, a lack of knowledge about the physiological changes to genetically defined circuits that arise from binge drinking is a major impediment to developing better treatment strategies. Since the extended amygdala is a heterogeneous structure that contains a variety of neuropeptides and neurotransmitters a deeper understanding of the component circuits and their response to alcohol is required to explain how alcohol fuels the negative affective component of addiction as well to devise novel strategies for therapeutic intervention.

The CeA is the primary output nucleus of the amygdala and is comprised of predominantly GABAergic projection neurons, which contain many different neuropeptides including neuropeptide Y (NPY), dynorphin and CRF[4,5]. CRF is a 41 amino acid neuromodulator that regulates stress and reward[6], and is often colocalized with other neurotransmitters including glutamate and GABA[7–9]. CRF cell bodies are present in the extended amygdala including the CeA and bed nucleus of the stria terminalis (BNST) and release CRF through 2 Gs-coupled postsynaptic receptors, CRF1 and CRF2. Furthermore, CRF binding protein (CRF-BP) is thought to “buffer” synaptically released CRF[10]. The presence of these stress and anti-stress neuropeptides link the CeA to anxiety-like behavior and AUDs such as binge drinking[11]. Indeed, both acute and chronic ethanol increase CeA GABAergic neurotransmission[12], and inactivation of CeA neuronal ensembles in alcohol dependent rats reduces binge drinking[13]. Moreover, CeA

neurons containing CRF are implicated in the modulation of binge drinking. Therefore, the role of CRF neurons in binge drinking remains particularly interesting in regards to their precise activity during acute and repeated binge drinking. Notably, increased CRF immunoreactivity within the CeA is observed after excessive alcohol administration, which remains elevated for several days following binge drinking[14]. Furthermore, administration of CRF compounds within the CeA reduces excessive drinking in rodents[14–16]. The above-mentioned data provides strong, presumptive evidence that binge drinking can regulate CeA CRF activity. However, knowledge of the precise activity of these neurons during binge drinking is lacking. For this reason, here, we used optogenetics coupled with *in vivo* electrophysiology to examine the activity of CeA CRF neurons during acute and chronic binge ethanol exposure. We found that CeA CRF neurons show heterogeneity in response to a lick of ethanol and an increase in activity in response to repeated binge drinking sessions.

Methods

Animals

$Crh^{tm1(cre)Zjh}$ mice (N=12) expressing Cre recombinase under the corticotropin-releasing hormone gene (Crh) promotor were obtained from the Jackson Laboratory. They shall be referred to as corticotropin-releasing factor – cre (CRF-Cre) mice herein. All mice were heterozygous and generated by mating a male homozygous CRF-Cre mouse with a female wildtype C57. All mice were placed in a reverse light/dark 3 weeks before any manipulation and maintained there during the entire experiments. All experiments were conducted in accordance with the United States National Research Council *Guide for the Care and Use of Laboratory Animals* and were approved by the University of Maryland School of Medicine Institutional Animal Care and Use Committee.

Optical-Fiber-Coupled Microelectrode arrays (OptoArrays)

Custom-made microelectrode arrays (MEA) were obtained from Innovative Neurophysiology (Durham, NC). The MEAs had 16 x 35 μm tungsten electrodes in a U-shape around a central pore for optical fibers. The MEA connector was offset from the center in a chair-like configuration to allow for the optical fiber.

Implantable optical fibers were fashioned in-house[17]. Briefly, 0.48 NA 200/230 μm optical fiber was stripped and affixed with a ceramic ferrule (235 μm ID, as above) and polished. Percent transmittance (%T) of the implants were calculated using an optical power meter (PM20A, ThorLabs) and fibers with <75 %T were discarded. Fiber implants were attached to the MEA approximately 500 μm (300-800 μm) dorsal to the tips of the electrodes, at a slight angle toward the electrodes. The fibers and MEA were encased in dental cement (Industrial Grade Grip Cement, powder #675571, liquid #675572, Dentsply, York, OA).

Survival Surgeries

At 8-12 weeks of age, CRF-Cre mice (N=12) were anesthetized with isoflurane via an E-Z Anesthesia brand vaporizer (E-Z Anesthesia, Palmer, PA). A craniotomy above the CeA was centered at -1.1mm A/P, +/-2.95mm L/M (from bregma) and was extended into a concentric square +/-0.25mm A/P and +/-0.25mm L/M. An adeno-associated viral vector (serotype 5) containing a double inverted open reading frame with the ChR2(h134R)-EYFP construct (AAV-EF1a-DIO-hChR2(H134R)-EYFP-WRE-Pa was purchased from the University of North Carolina's Vector Core, with permission from Karl Deisseroth. The virus was infused into the CeA via a Hamilton 7001 1-μL syringe (Hamilton Company, Reno, NV), which was inserted into a Micro4 microinfusion pump (UMC4 controller, UMP3 pump; World Precision Instruments, Sarasota, FL). The needle was slowly lowered -4.85 mm D/V (from brain surface) into the brain and 500nl of the virus was infused at 100nl/min. After 5-minutes, the needle was slowly removed and the optoarrays were implanted. Optoarrays were secured to the skull using anchor

screws (MF-5182 bone screws; Bioanalytical Systems, Inc, West Lafayette, IN), with the ground wire wrapped around one screw and inserted 2 mm into the cerebellum. The array was then encased in a dental cement headcap (Industrial Grade Grip Cement, powder #675571, liquid #675572, Dentsply, York, OA).sd

Following surgery, the mice recovered for two weeks before starting the drinking protocol. Following surgery, all mice were singly housed. At the completion of the experiment, mice were euthanized and brains were processed for histology. We passed a high current electrical signal through the head cap to check for placements. All surgical procedures were approved by the University of Maryland, Baltimore IACUC committee.

Alcohol Consumption Protocol

Mice underwent several weeks of a modified version of the drinking-in-the-dark (DID) protocol. Briefly, 3 hours into the dark phase of their light-cycle, mice were placed into a chamber with a water bottle filled with 20% ethanol (in tap water) and food. Mice remained in the chamber for 4 hours and the number of licks and weight of alcohol consumed were analyzed. Mice were run for 4 consecutive days followed by 3 days of abstinence. Each mouse had 5 cycles of binge drinking (20 total binge drinking days over 5 weeks). Licks were quantified by the current passed when a mouse's tongue completed the circuit between the metal floor grid and metal sipper of the ethanol bottles.

Recording Hardware

In vivo electrophysiology recordings were performed using an Omniplex-DHP system from Plexon, Inc (Dallas, TX), with a motorized commutator from NeuroTek (Toronto, Ontario, Canada). The wideband signal was acquired at 40kHz, with an analog high-pass filter of 7.5Hz, and a 7.5kHz low pass filter before the signal was digitized at the headstage. The continuous spike data were extracted from the wideband signal by applying a 4-pole 500Hz Butterworth

high pass filter and a 4-pole 3000Hz Butterworth low pass filter. Common median referencing was used for all recording sessions.

Optical Identification of Genetically-Defined Neurons (Phototagging)

Opto-array mice were tethered to a headstage and mini patch cord with ferrules on both ends plugged onto the fiber implant of the optoarray and bound to the headstage cables. The other end of the mini-patch cord remained unplugged for the duration of the 4-hour drinking session. After the DID session, the mini patch chord attached to the mouse was then connected to the laser-attached patch chord and the phototagging procedure began. Phototagging was done in accordance with previous reports[18]. At the end of the recording session, mice received a series of stimulation patterns at 1, 5, 10, and 20 Hz (20 4-ms long pulses each).

We defined a unit as a putative CRF neuron only when all criteria for phototagging were fulfilled: a significant increase in firing rate within 10ms after the beginning of a light pulse, when compared to the 10 ms prior to the event (as identified by a Wilcoxon signed rank test on the binned spike/sec data); the light-evoked waveforms had to have a cross-correlational coefficient R >0.9 when compared to the naturally occurring waveforms. Units were classified as light-excited, light-inhibited or no response, using Wilcoxon signed rank tests on time bins before and after the event.

Lick Response Type Classification

To classify the encoding pattern for each unit in relation to licking, we calculated peri-event raster plots and histograms for all units, from -100ms to +100ms, using 5ms bins, with licks centered at time 0s. We analyzed the average firing rates in 50ms periods before and after licking (Baseline: -100ms to -50ms; Pre-Lick: -50ms to 0ms; Post-Lick:0ms to +50ms). We performed Wilcoxon rank-sign tests on these firing rates and classified the response types based on which of these comparisons were significantly different and the sign of the difference

between averages. We identified four types of lick-responses: lick-excited (E), lick-inhibited (I), lick-predictive (P), and no response (NR) (see Table 1 for detailed classification criteria).

TYPE	Pre-Lick - Baseline	Post-Lick – Pre-Lick
Excited (E)	No change	Sig. increase
Inhibited (I)	No change	Sig. decrease
Predictive (P)	Sig. increase	Sig. increase
No Response (NR)	No change	No change

Burst-Firing Definition and Classification

We identified the beginning of a burst as a series of at least two spikes with an interspike-interval less than 50ms and its end when the interspike-interval exceeded 100ms. Furthermore, units were classified based on their firing rate and % of spikes in bursts (%SiB), as previously reported [19,20], but with revised criteria according to the distribution of firing rate and %SiB for these neurons. We applied a cutoff of 4Hz for the firing rate and 30% for the %SiB. We identified 4 types: low-firing/high-burst (LFHB), low-firing/low-burst (LFLB), high-firing/high-burst (HFHB), and high-firing/low-burst (HFLB).

Data Processing and Analysis

Plexon OfflineSorter 4 was used to process and separate identified units from each recording. Units from the same electrode were considered different as long as the waveforms were significantly separated in 3D principal component space as tested by multivariate ANOVA ($p<.05$), with L-ratios <0.05 for each cluster. Units were classified based upon their responses to light stimulation, and licks

Outlier Time Bin Removal and Replacement

In order to eliminate any large fluctuations in noise that may have contaminated individual time bins out of the 4-hour recordings, we first calculated raw firing rate in 5-minute bins. We then used the Matlab function filloutliers to identify and replace outlier time bins, as identified using a sliding window 6 time-bins-wide (30mins) to calculate the median, and any bins that were more than 3 scaled deviations away from the median were identified as outliers and substituted with a linear interpolation of the time bins surrounding the outlier. This was done prior to the baseline subtracted firing rate z-score calculation. The same outlier time bins were also used to remove outlier time bins for burst firing metrics from correlation analyses.

Statistics

All data were presented as means ± SEM and analyzed using GraphPad Prism 7 and Matlab 2017. Comparisons between CRF and non-CRF units were analyzed using Mann-Whitney U tests. Comparisons between 3 unit types were analyzed using Kruskal-Wallis tests with *post-hoc* Dunn's multiple comparison tests. All comparisons across hours were done using two-way repeated measures ANOVA with *post-hoc* Sidak's multiple comparison tests for between-group comparisons and *post-hoc* Tukey's multiple comparison tests. Comparisons between early and late ethanol session correlations were analyzed using Kolmogorov-Smirnov tests.

Results

Identification and electrophysiological profile of CRF vs non-CRF neurons

Opto-arrays recorded from optically identified CRF neurons within the CeA during binge drinking behavior sessions (**Fig 1 A, B**). We analyzed 149 units, of which 59 were classified as putative CRF units, 75 non-light-responsive, 4 light-excited (we observed spiking approx. 10 ms after

optical stimulation, hence we theorize that this group are not CRF positive, and 11 light-inhibited (**Fig 1 C**). Herein, we refer to non-light-responsive units as non-CRF neurons and phototagged units as putative CRF neurons. Due to their higher prevalence, we focused our analyses on these two categories. We evaluated several electrophysiological parameters (**Fig 1 D**) and found that CRF neurons had significantly higher firing rates and burst rates, and smaller coefficients of variation (an index of firing regularity) when compared to non-CRF units (**Fig 1 D**)**.**

CeA-CRF neurons have distinct firing characteristics in response to a lick of ethanol

Since the CeA CRF system is engaged by excessive ethanol drinking, we then examined whether CRF units encoded voluntary consumption of alcohol, using licking as our behavioral index. CRF-Cre mice steadily drank more during 4-hour sessions (**Fig 2A, left**). They also developed a robust increase in licking for ethanol over repeated sessions compared to water (**Fig 2A, right**).

We next determined if CRF unit firing activity was correlated with ethanol licking. We therefore compared CRF vs non-CRF units during early ethanol sessions (session #1-8) versus late sessions (session # 17+). We found that only CRF units significantly increased the strength of their correlation in late sessions compared to early sessions (**Fig 2B**).

To ascertain if CRF units encoded ethanol consumption, we analyzed peri-event histograms for each unit (see General Methods for lick-response-type classification). We identified four types of lick-responses: lick-excited (CRF-E), lick-inhibited (CRF-I), lick-predictive (CRF-P), and no response (CRF-NR) (**Fig 2 C**). We focused our analyses on the two most prevalent types, CRF-P and CRF-NR (which represented 86.4% of all CRF units, **Fig 2 D**), including non-CRF non-lick responsive (non-CRF-NR) as a control group.

We found that CRF-P neurons had a significantly higher firing rate, as well as the percentage of spikes in bursts (%SiB), burst duration, burst rate, and # of spikes per burst compared to both CRF-NR or non-CRF-NR units (**Fig 2E**), suggesting that CRF-P cells were more active during alcohol consumption.

CRF-P units increase firing activity throughout drinking sessions

We compared the change in firing rate within-sessions between CRF-P and CRF-NR neurons, using Z-scores normalized to the first 30 minutes as baseline (**Fig 3 A**). We found a significant difference among CRF types, which diverged for hours 3 and 4, with CRF-P units displaying higher firing rates (**Fig 3 B, top**)**.** Next we analyzed the effect of firing rate vs session-hour for each CRF type alone, post hoc tests revealed CRF-P units increased firing rates within-session, whereas CRF-NR cells did not (**Fig 3 B, top panels**). We also compared changes in %SiB within-session, but there was no effect of session-hour, but a significant difference between CRF types, with CRF-P neurons showing higher %SiB (**Fig 3 B, bottom panels**). Thus, CRF-P units changed firing rate dynamically during ethanol sessions, while bursting activity remains consistently higher throughout ethanol sessions.

CRF lick-response types show heterogeneous changes in firing activity

When we ranked each CRF cell type by the change in firing rates from hour 1 to hour 4 (Δ-rate) (**Fig 3 A-C**) we found that each CRF cell type had two sub-groups, with either increased firing rates (Δ+) or decreased (Δ-). Hence, we split each CRF-NR and CRF-P units into two sub-groups: CRF-NR(Δ+), CRF-NR(Δ-), CRF-P(Δ+), and CRF-P(Δ-) and compared the Δ-rate within sub-groups as follows: CRF-NR(Δ+) vs. CRF-NR(Δ-), and CRF-P(Δ+) vs CRF-P(Δ-), revealing that the Δ-rate sub-groups were indeed significantly distinct groups for both CRF-NR and CRF-P units (**Fig 3 C, left, orange vs blue bars**). Additionally, CRF-P(Δ+) units increased rate significantly more than CRF-NR(Δ+) cells, but there was no significant difference between the

decrease in rates of CRF-P(Δ-) and CRF-NR(Δ-) (**Fig 3 C, left**). Therefore, to further investigate these changes, we analyzed the normalized firing rates for all 4 sub-types (**Fig 3 C, right**).

First we compared changes in firing rate between sub-groups over the full session, using average normalized firing rate and %SiB by hour (**Fig 3 D**). We found that CRF-P(Δ+) unit activity increased steadily and was robustly higher by hours 3 and 4 while CRF-P(Δ-) cells showed no significant change throughout the session (**Fig 3D, top left**)**.** While CRF-(Δ+) units dynamically changed firing rate throughout the session, they showed only modest and inconsistent changes in %SiB, as only hour 1 and hour 3 were statistically distinct (**Fig 3 D, bottom left).** On the other hand, despite the firing rate of CRF-P(Δ-) neurons being independent of session time, we found that these units markedly decreased their %SiB throughout the session (**Fig 3 D, bottom left).**

Therefore, while CRF-P(Δ+) sub-groups showed a substantial rise in firing rate over the course of ethanol drinking sessions, accompanied by a modest increase in burst firing, CRF-P(Δ-) neurons did not change their overall firing rate across the session, but significantly decreased their bursting activity. Conversely, combined CRF-NR units did not significantly change firing rates during the session (**Fig 3B**), and both sub-groups showed only modest changes in firing rate (**Fig 3 D, top right)**. While CRF-NR(Δ+) neurons only increased rate by hour 4, CRF-NR(Δ-) units significantly decreased firing rate after hour 1 (**Fig 3D, top right**). When we analyzed the change %SiB, we found a similar pattern, with CRF-NR(Δ+) increasing %SiB by hour 4, and (Δ-) units decreasing %SiB for the final two hours (**Fig 3 D, bottom right)**. Interestingly, the changes in rate and %SiB for CRF-NR units were to a much smaller degree than those seen in CRF-P sub-groups.

Overall, we concluded that CRF-P units are adaptively responsive over the 4-hour drinking sessions, either by increasing firing rates as in the CRF-P(Δ+) or by decreased bursting

as in the CRF-P(Δ-) units. On the other hand, CRF-NR units modestly changed their firing rate and %SiB over the 4-hour sessions.

CRF-P units increase firing and bursting activity over repeated drinking sessions

Finally, we examined whether the firing activity of CRF neurons changed over repeated sessions of ethanol consumption. When we compared CRF lick-response types, we found that CRF-P units had much higher patterned firing rates in later sessions compared to early sessions, while CRF-NR units did not display any adaptive change in their firing rates in later drinking sessions (**Fig 4A**). We also examined the %SiB in early vs late sessions and found similar results, with only CRF-P cells showing a substantial increase in bursting in later sessions, while CRF-NR units displaying no change (**Fig 4B)**.

Altogether, this evidence further supports a relationship between prolonged/repeated ethanol consumption and the firing/burst properties of CRF neurons in the CeA. Moreover, a population of CeA-CRF units exists that fires immediately before the mouse responds for ethanol (CRF-P units), and these neurons dynamically modify their firing rate and %SiB during the 4-hour ethanol drinking sessions, as well as following repeated ethanol sessions.

Discussion

Chronic binge drinking often leads to the manifestation of alcohol use disorder (AUD)[21–24]. The central amygdala is identified as a critical brain region involved in mediating excessive binge ethanol drinking[13,25–27]. Particularly, histochemical and electrophysiological evidence suggests that binge drinking engages the CeA CRF system[16,28–30]. However, the functional dynamics of CeA CRF signaling during these behaviors have remained elusive. Here, we used optogenetic strategies coupled with *in vivo* electrophysiology to identify and record from CeA CRF neurons during acute and repeated binge drinking sessions in mice. Since CeA CRF neurons cannot be identified by waveform characteristics in traditional electrophysiology

experiments, we identified them by measuring spike latency after photostimulation *in vivo*. All photostimulations occurred at the end of each ethanol session to avoid unintended excitation during the behavioral experiments[18]. Using our latency cutoff time of 5 ms, we should not be recording non CRF neurons due to downstream trans synaptic activation. Approximately 39% of all CeA neurons recorded were identified as putative CRF cells. First, we compared identified CRF neurons to other recorded neurons in the CeA from our entire binge drinking recording sessions. We found that CeA CRF neurons exhibit increased firing and bursting activity compared to non-light responsive CeA neurons. Since it is hypothesized that multiple alcohol exposure enhances CeA CRF neurons, this result may be due to our binge drinking paradigm, However, our experiments pooled all recorded units during the entire binge drinking experiment, therefore this may not provide an accurate representation of CeA CRF circuit dynamics. This is why we further analyzed these data to examine potential heterogeneity within these groups as well as the temporal dynamics of the effects observed.

Since CeA CRF neurons project to multiple brain areas including the bed nucleus of the stria terminalis, ventral tegmental area, and periaqueductal grey, it was parsimonious that we observed a heterogenous population within our CeA CRF neurons. Therefore, we subdivided the CeA CRF population based on their firing rate in response to a lick of ethanol. The vast majority of CeA CRF were either predictive (P) or exhibited no effect (NR) with only smaller numbers within the inhibition (I) and excitation (E) groups. Next, we examined plastic changes of CRF (P), (NR), and non CRF cells within the CeA after binge ethanol drinking. CRF (P) neurons were more excitable than CRF (NR) and non CRF neurons. It is hypothesized that CeA CRF neurons project to the VTA, so it is possible that the majority of CRF (P) cells may project to the VTA. Since CRF is colocalized with GABA in the CeA, we speculate that ethanol activates VTA projecting CeA CRF neurons resulting in the release of GABA onto VTA GABAergic neurons. Thus, VTA dopamine could be enhanced due to decreased VTA GABA drive onto VTA

dopamine neurons. Furthermore, we speculate that the increased bursting activity observed is due to increased probability of CRF peptide release from CeA neurons. Future studies are necessary to determine whether peptide release can be observed with phasic high frequency stimulation patterns.

As described above, CRF (P) neurons exhibited significant increases in firing rates when compared to CRF (NR) neurons. However, with further analyses we observed a biphasic distribution in the CRF (P) and the CRF (NR) cells during our ethanol sessions. In both groups we found that one subpopulation significantly increased their firing as the mouse consumed more ethanol, while the other one exhibited a decrease. These data further support our claims that CeA CRF neurons display heterogeneous responses to ethanol. This is important as a previous study examining CeA CRF used pharmacology to globally inhibit this area[16]. One drawback with these analyses was that all data were grouped together regardless of ethanol session. So consequently, our next set of analyses examined how acute and chronic binge ethanol consumption may modify the CeA CRF system.

To do this, we examined the activity of CRF (P) and CRF (NR) neurons during acute and repeated binge ethanol sessions. Studies reveal that repeated ethanol vapor administration results in excessive drinking, which is blocked by CeA CRF compounds[14,15,31]. Moreover, chronic intermittent ethanol vapor leads to an upregulation of CRF and CRF1 receptor mRNA[32]. These data provide strong presumptive evidence that chronic ethanol administration can hijack the CeA CRF system leading to greater maladaptive neuronal plasticity. Critically, we observed that only CRF (P) neurons increased their firing rate and burst activity during binge drinking cycles. This effect was not observed in CRF (NR) neurons. Future experiments should examine if the activity of CeA CRF neuron following water or natural reward consumption follows the same adaptive patterns

In conclusion, we identified a diverse role of CeA CRF neurons in response to binge drinking. These data make a strong case that genetically identical neurons within a structure are heterogenous and complex. It bears the caveat that optogenetic and/or pharmacological manipulation of identical groups of neurons may provide a false positive in regard to behavior. Future studies should examine the role of circuits and activity dependent groups of neurons for a more dissected analysis of behaviorally relevant patterns of activity.

Funding and Disclosure: This work was supported by NIH/NIAAA grant R00 AA021417 (D. R. S.). The authors declare no competing interests

Acknowledgments: We thank Dr. Brian Mathur and Dr. Joe Cheer for discussion. We thank Colin Maehler, Houman Qadir, and Soham Roy for their technical assistance.

References

1. Sacks, J. J., Gonzales, K. R., Bouchery, E. E., Tomedi, L. E. & Brewer, R. D. 2010 National and State Costs of Excessive Alcohol Consumption. *Am. J. Prev. Med.* **49**, e73–e79 (2015).
2. Bonomo, Y. A., Bowes, G., Coffey, C., Carlin, J. B. & Patton, G. C. Teenage drinking and the onset of alcohol dependence: a cohort study over seven years. *Addict. Abingdon Engl.* **99**, 1520–1528 (2004).
3. Koob, G. F. & Le Moal, M. Review. Neurobiological mechanisms for opponent motivational processes in addiction. *Philos. Trans. R. Soc. Lond. B. Biol. Sci.* **363**, 3113–3123 (2008).
4. Sah, P. & Lopez De Armentia, M. Excitatory synaptic transmission in the lateral and central amygdala. *Ann. N. Y. Acad. Sci.* **985**, 67–77 (2003).
5. Sah, P., Faber, E. S. L., Lopez De Armentia, M. & Power, J. The amygdaloid complex: anatomy and physiology. *Physiol. Rev.* **83**, 803–834 (2003).
6. Rivier, J., Spiess, J. & Vale, W. Characterization of rat hypothalamic corticotropin-releasing factor. *Proc. Natl. Acad. Sci. U. S. A.* **80**, 4851–4855 (1983).
7. Wise, R. A. & Morales, M. A ventral tegmental CRF-glutamate-dopamine interaction in addiction. *Brain Res.* **1314**, 38–43 (2010).
8. Tagliaferro, P. & Morales, M. Synapses between corticotropin-releasing factor-containing axon terminals and dopaminergic neurons in the ventral tegmental area are predominantly glutamatergic. *J. Comp. Neurol.* **506**, 616–626 (2008).
9. Merchenthaler, I., Vigh, S., Petrusz, P. & Schally, A. V. Immunocytochemical localization of corticotropin-releasing factor (CRF) in the rat brain. *Am. J. Anat.* **165**, 385–396 (1982).
10. Behan, D. P. *et al.* Neurobiology of corticotropin releasing factor (CRF) receptors and CRF-binding protein: implications for the treatment of CNS disorders. *Mol. Psychiatry* **1**, 265–277 (1996).
11. Gilpin, N. W., Herman, M. A. & Roberto, M. The Central Amygdala as an Integrative Hub for Anxiety and Alcohol Use Disorders. *Biol. Psychiatry* **77**, 859–869 (2015).

12. Roberto, M., Gilpin, N. W. & Siggins, G. R. The central amygdala and alcohol: role of γ-aminobutyric acid, glutamate, and neuropeptides. *Cold Spring Harb. Perspect. Med.* **2**, a012195 (2012).
13. Guglielmo, G. de *et al.* Recruitment of a Neuronal Ensemble in the Central Nucleus of the Amygdala Is Required for Alcohol Dependence. *J. Neurosci.* **36**, 9446–9453 (2016).
14. Finn, D. A. *et al.* Increased drinking during withdrawal from intermittent ethanol exposure is blocked by the CRF receptor antagonist D-Phe-CRF(12-41). *Alcohol. Clin. Exp. Res.* **31**, 939–949 (2007).
15. Funk, C. K., O'Dell, L. E., Crawford, E. F. & Koob, G. F. Corticotropin-releasing factor within the central nucleus of the amygdala mediates enhanced ethanol self-administration in withdrawn, ethanol-dependent rats. *J. Neurosci. Off. J. Soc. Neurosci.* **26**, 11324–11332 (2006).
16. Lowery-Gionta, E. G. *et al.* Corticotropin releasing factor signaling in the central amygdala is recruited during binge-like ethanol consumption in C57BL/6J mice. *J. Neurosci. Off. J. Soc. Neurosci.* **32**, 3405–3413 (2012).
17. Sparta, D. R. *et al.* Construction of implantable optical fibers for long-term optogenetic manipulation of neural circuits. *Nat. Protoc.* **7**, 12–23 (2012).
18. Cohen, J. Y., Haesler, S., Vong, L., Lowell, B. B. & Uchida, N. Neuron-type-specific signals for reward and punishment in the ventral tegmental area. *Nature* **482**, 85–88 (2012).
19. Scheggi, S. *et al.* PPARα modulation of mesolimbic dopamine transmission rescues depression-related behaviors. *Neuropharmacology* **110**, 251–259 (2016).
20. Mameli-Engvall, M. *et al.* Hierarchical Control of Dopamine Neuron-Firing Patterns by Nicotinic Receptors. *Neuron* **50**, 911–921 (2006).
21. Kranzler, H. R. & Soyka, M. Diagnosis and Pharmacotherapy of Alcohol Use Disorder: A Review. *JAMA* **320**, 815–824 (2018).
22. Ferguson, L. B. *et al.* Dissecting Brain Networks Underlying Alcohol Binge Drinking Using a Systems Genomics Approach. *Mol. Neurobiol.* (2018). doi:10.1007/s12035-018-1252-0

23. Dawson, D. A., Grant, B. F. & Li, T.-K. Quantifying the risks associated with exceeding recommended drinking limits. *Alcohol. Clin. Exp. Res.* **29**, 902–908 (2005).
24. Rehm, J. *et al.* The relation between different dimensions of alcohol consumption and burden of disease: an overview. *Addict. Abingdon Engl.* **105**, 817–843 (2010).
25. Cozzoli, D. K. *et al.* Binge alcohol drinking by mice requires intact group 1 metabotropic glutamate receptor signaling within the central nucleus of the amygdala. *Neuropsychopharmacol. Off. Publ. Am. Coll. Neuropsychopharmacol.* **39**, 435–444 (2014).
26. Lee, K. M., Coehlo, M., McGregor, H. A., Waltermire, R. S. & Szumlinski, K. K. Binge alcohol drinking elicits persistent negative affect in mice. *Behav. Brain Res.* **291**, 385–398 (2015).
27. Olney, J. J., Navarro, M. & Thiele, T. E. The Role of Orexin Signaling in the Ventral Tegmental Area and Central Amygdala in Modulating Binge-Like Ethanol Drinking Behavior. *Alcohol. Clin. Exp. Res.* **41**, 551–561 (2017).
28. Gilpin, N. W., Karanikas, C. A. & Richardson, H. N. Adolescent binge drinking leads to changes in alcohol drinking, anxiety, and amygdalar corticotropin releasing factor cells in adulthood in male rats. *PloS One* **7**, e31466 (2012).
29. Gilpin, N. W. & Roberto, M. Neuropeptide modulation of central amygdala neuroplasticity is a key mediator of alcohol dependence. *Neurosci. Biobehav. Rev.* **36**, 873–888 (2012).
30. Karanikas, C. A., Lu, Y.-L. & Richardson, H. N. Adolescent drinking targets corticotropin-releasing factor peptide-labeled cells in the central amygdala of male and female rats. *Neuroscience* **249**, 98–105 (2013).
31. Koob, G. & Kreek, M. J. Stress, dysregulation of drug reward pathways, and the transition to drug dependence. *Am. J. Psychiatry* **164**, 1149–1159 (2007).
32. Eisenhardt, M., Hansson, A. C., Spanagel, R. & Bilbao, A. Chronic intermittent ethanol exposure in mice leads to an up-regulation of CRH/CRHR1 signaling. *Alcohol. Clin. Exp. Res.* **39**, 752–762 (2015).

Figure Legends

Figure 1. Optical identification of CRF neurons *in vivo.* **A)** Scaled diagram of optical-fiber coupled microarray implanted into the central amygdala of CRF-cre mice, and local CeA injection of AAV-DIO –Channelrhodopsin2-EYFP virus, whose expression is showed in the image. **B)** Peristimulus time histogram and scatter plot showing identified CRF neurons. Units were classified as CRF only if they fired within 10 ms of the onset of a 4 ms-long light pulse, and the light-evoked waveforms had an R^2 >0.9 compared to non-light evoked waveforms. **C)** The pie chart shows that out of 149 total units, 59 were identified as putative CRF neurons, 75 non-responsive to light, and a small population excited (4) or inhibited (11). Due to the low n for these light responses, we focused on CRF units vs non-light-responsive units, herein "NonCRF". **D)** Electrophysiological characterization of CRF vs non-CRF neurons. Graphs showing firing rate, coefficient of variation, % of spikes in bursts (%SiB), burst duration, intraburst frequency, and burst rate. Error bars are standard error of the mean (SEM). We found CRF units had a higher firing rate (U=1589, p=.005), a smaller coefficient of variation (U=1488, p=.0011), and a higher burst rate (U=1770, p=.0469) when compared to non-CRF units. **p<.01, *p<.05, Mann-Whitney test. La = lateral amygdaloid nucleus. ec = external capsule. CeC = lateral capsular part of the central nucleus of the amygdala (CeA). CeL, CeM= lateral and medial subdivision of the CeA, respectively.

Figure 2. CRF Neurons encode licking-behavior. **A, Left)** Average cumulative licks during a drinking session for all recorded sessions (N=12 mice). **A, right)** Graph of representative number of licks over repeated ethanol sessions in a different cohort of mice (N=24 mice). **B)** Graphs show that overall, CRF units (n=37) had a significant shift in their correlation values for firing rate vs cumulative licks from early to late sessions (early CRF (n=20), late CRF (n=17); D=0.4804, p=.0134) whereas non-CRF units did not (early NonCRF (n=41), late NonCRF (n=

34); D=0.2267, p=.2951). *p<.05, Kolmogorov-Smirnov test. **C)** Perievent Raster plots for representative units for each lick-response type. Units were classified into 4 lick-response types, based upon changes in firing rates during 3 time periods: baseline (-100 ms to -50 ms before licks) vs. pre-lick (-50 ms to 0ms), post-lick (0 ms to +50 ms). Wilcoxon signed-rank tests were performed on pairs of these time periods to determine if there were significant changes in firing rates from baseline to pre-lick and from pre-lick to post-lick. **D)** The pie chart indicates that out of our 59 CRF units, 6 were lick-excited (CRF-E), 2 were lick-inhibited (CRF-I), 24 were lick-predictive (CRF-P), and 27 showed no response (CRF-NR). Due to the low number of CRF-E and CRF-I units, we focused on the two major response classes, CRF-NR and CRF-P. **E)** Graph show electrophysiological parameters such as firing rate, coefficient of variation, %SiB, burst duration, intraburst frequency, burst rate and # of spikes per burst, of CRF-NR, CRF-P, and non-CRF NR (included as a control). CRF-P units had a higher firing rate (H=16.43, p=.0003), %SiB (H=12.55, p=.0019), burst duration (H=14.09, p=.0009), burst rate (H=16.8, p=.0002), and # of spikes per burst (H=11.45, p=.0033) than CRF-NR and non-CRF-NR units. Furthermore, CRF-NR cells showed a lower coefficient of variation when compared to non-CRF-NR (H=9.492, p=.0087). ***p<.001, **p<.01, *p<.05, Kruskal-Wallis H-test with Dunn's multiple comparisons test.

Figure 3. CRF-P Neurons increase firing activity during ethanol sessions, with heterogeneous sub-types. **A)** Normalized Firing Rate Z-Scores were calculated using the first 30 mins as the baseline period for calculating the mean and std used to calculate Z-scores for the full-session. Z-scores are shown in color, with each horizontal line is one unit's activity for the 4-hour drinking session. Units are grouped by lick-response type and then ordered from top-bottom by rate change (hour 4 – hour 1). **B) Left**: Average normalized firing rates and %SiB calculated in 5 min bins. **Right**: Hourly averages of the same activity used for statistical analysis. **Right, top:** CRF-P units had a higher firing rate vs CRF-NR units (main effect of CRF type: $F_{(1, 49)}$ = 7.957,

p=.0069; hour: $F_{(3, 147)}$ = 2.545, p=.0583; CRF-type by hour interaction ($F_{(3, 147)}$ = 3.924, p=.0099). **p<.01, 2way ANOVA. Post-hoc tests show that CRF-P units increased throughout the session with significantly higher rates by hours 3 and 4 ($^{\alpha\alpha}$p<.01, $^{\alpha}$p<.05, Tukey's tests), whereas CRF-NR did not change across hours. **Right, bottom:** CRF-P units also had higher % of spikes in bursts ($F_{(1, 49)}$ = 21.6, p<.0001), but did not change over the session ($F_{(3, 147)}$ = 1.775, p=.1545). ****p<.0001, 2way ANOVA. **C) Left:** Pie charts and bar graphs show how units were sorted by change in firing rate (hour 4 – hour 1). CRF-NR and CRF-P were separated into two statistically different subtypes that increased firing rate (Δ+) and decreased rate (Δ-) respectively (ethanol response: $F_{(1, 46)}$ = 7.019, p=.0110; CRF-type: $F_{(1, 46)}$ = 55.06, p<.0001). ****p<.0001, ***p<.001, *p<.05, Sidak's multiple comparison test. **Right:** The average normalized firing of each CRF sub-types: CRF-NR(Δ+) (n=8), CRF-NR(Δ-) (n=19), CRF-P(Δ+) (n=9), CRF-P(Δ-) (n=14). **D**) **Left, top**: CRF-P(Δ-) and CRF-P(Δ+) firing rates were significantly distinct ($F_{(1, 22)}$ = 32.86, p<.0001) for hours 3 and 4 (Sidak's test: ****p<.0001). CRF-P(Δ+) increased throughout the sessions with hours 1 and 2 distinct from 3 and 4 ($^{¤¤¤¤}$p<.0001, $^{¤¤¤}$p<.001, Tukey's tests), but CRF-P(Δ-) did not change. **Left, bottom**: CRF-P subtypes had a significantly different change in %SiB for hours 2-4 ($F_{(1, 22)}$ = 22.73, Sidak's test: ****p<.0001) with a significant hour by sub-type interaction ($F_{(3, 66)}$ = 11.98, p<.0001). CRF-P(Δ+) changed from hour 1 vs hour 3($^{€}$p<.05, Tukey's test), whereas CRF-P(Δ-) changed from hour 1 vs 2-4 ($^{\$\$\$\$}$p<.0001, $^{\$\$}$p<.01, $^{\$}$p<.05, Tukey's tests). **Right, top:** CRF-NR(Δ+) and CRF-NR(Δ-) were significantly different ($F_{(1, 26)}$ = 34.41, p<.0001) for hours 2-4 (Sidak's test: ****p<.0001, **p<.01). CRF-NR(Δ+) increased firing rate by hour 4 vs hours 1-3 (Tukey's tests: ####p<.0001). CRF-NR(Δ-) had lower firing rates in hours 2-4 vs hour 1 (Tukey's test: ‡‡‡‡p<.0001, ‡‡p<.01). **Right, bottom:** While CRF-NR subtypes did not have a significant main effect of sub-type ($F_{(1, 25)}$ = 3.071, p=.0920) or hour ($F_{(3, 75)}$ = 0.9743, p=.4095), there was a significant sub-type by hour interaction ($F_{(3, 75)}$ = 7.535, p=.0002). Post-hoc tests show that CRF-NR(Δ-) units decreased

%SiB from hour 1 to hours 3 and 4 (Tukey's tests: $^{§§§}p<.001$, $^{§}p<.05$) and CRF-NR(Δ+) units increased from hours 1 and 2 to hour 4 (Tukey's tests: $^{†}p<.05$).

Figure 4. Changes in CRF activity over repeated ethanol sessions. **A)** CRF-P increased raw firing rates after repeated ethanol sessions (main effect of ethanol session: $F_{(1, 38)} = 11.34$, p=.0017; main effect of CRF type: $F_{(1, 38)} = 13.85$, p=.0006; Tukey's tests: Early vs Late CRF-P: ***p=.0005), which was absent in CRF-NR units (Tukey's tests: Early vs Late CRF-NR: p=.9986). **B)** Similarly, CRF-P units showed a significant increase in the %SiB after repeated ethanol sessions (main effect of CRF-type: $F_{(1, 38)} = 12.44$, p=.0011, ethanol session: $F_{(1, 38)} = 7.138$, p=.0111; Tukey's tests: Early vs Late CRF-P: **p=.0029) and CRF-NR did not (Tukey's tests, p=.9961).

Supplemental Figure 1. We further analyzed the firing/burst properties of the units neurons by classifying them into four different groups (using a cutoff of firing rate to 4 Hz, and burst firing to 30%. The four classes were low firing/high burst (LFHB), high firing/high burst (HFHB), low firing/low burst (LFLB), and high firing/low burst (HBLB). **A)** Example spike trains and autocorrelograms from representative units of each class. **B)** Units plotted as %SiB vs firing rate. The horizontal dashed line marks the cutoff between low and high bursting (cutoff=30%), and the vertical dashed line marks the cutoff between low and high firing (cutoff=4 Hz). **C)** Population distributions for the burst-firing class for the lick-response types of interest. CRF-P had approximately 26% of LFHB, 23% of HFHB, and 50% of LFLB, whereas CRF-NR showed a low % of LFHB (7%), no HFHB, and a higher % of LFLB (~92%). NonCRF non-lick responsive (NR-NR) units had ~75% LFLB, and 25% LFHB, and a very low % of HFHB units (2%), indicating the HFHB class may be a defining characteristic for CeA-CRF-P units

Irving, Aroni, and Sparta 2018

Figure 1.

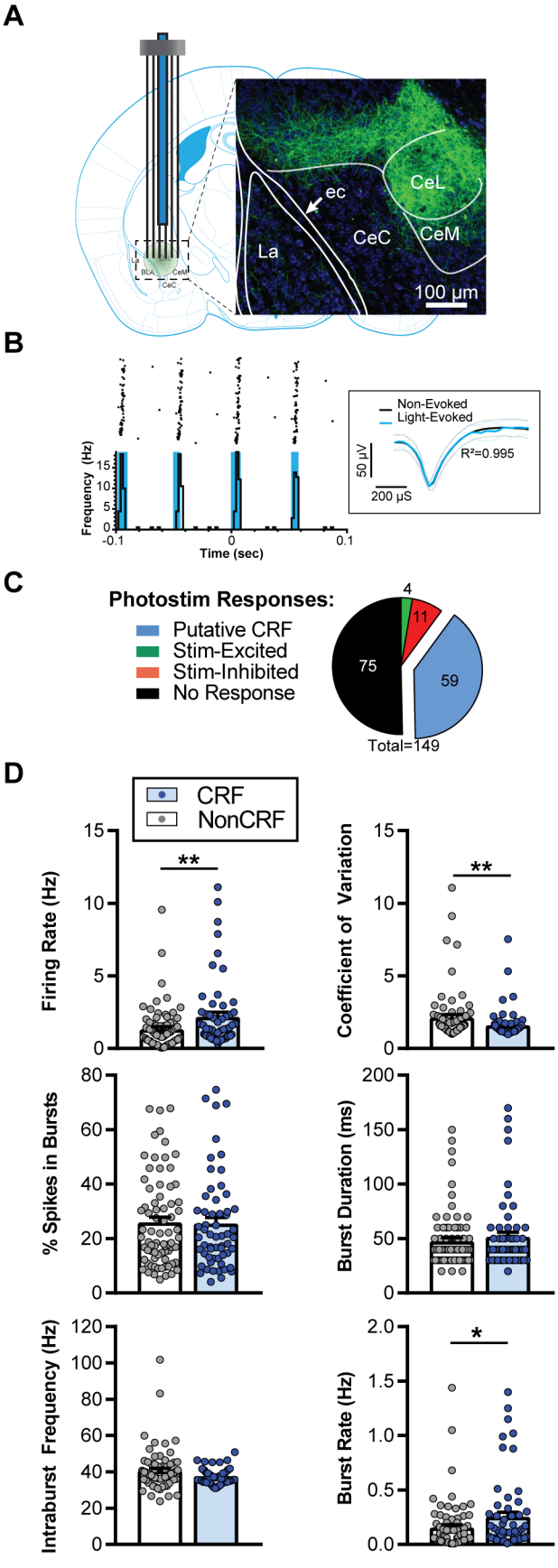

Irving, Aroni, and Sparta 2018

Figure 2

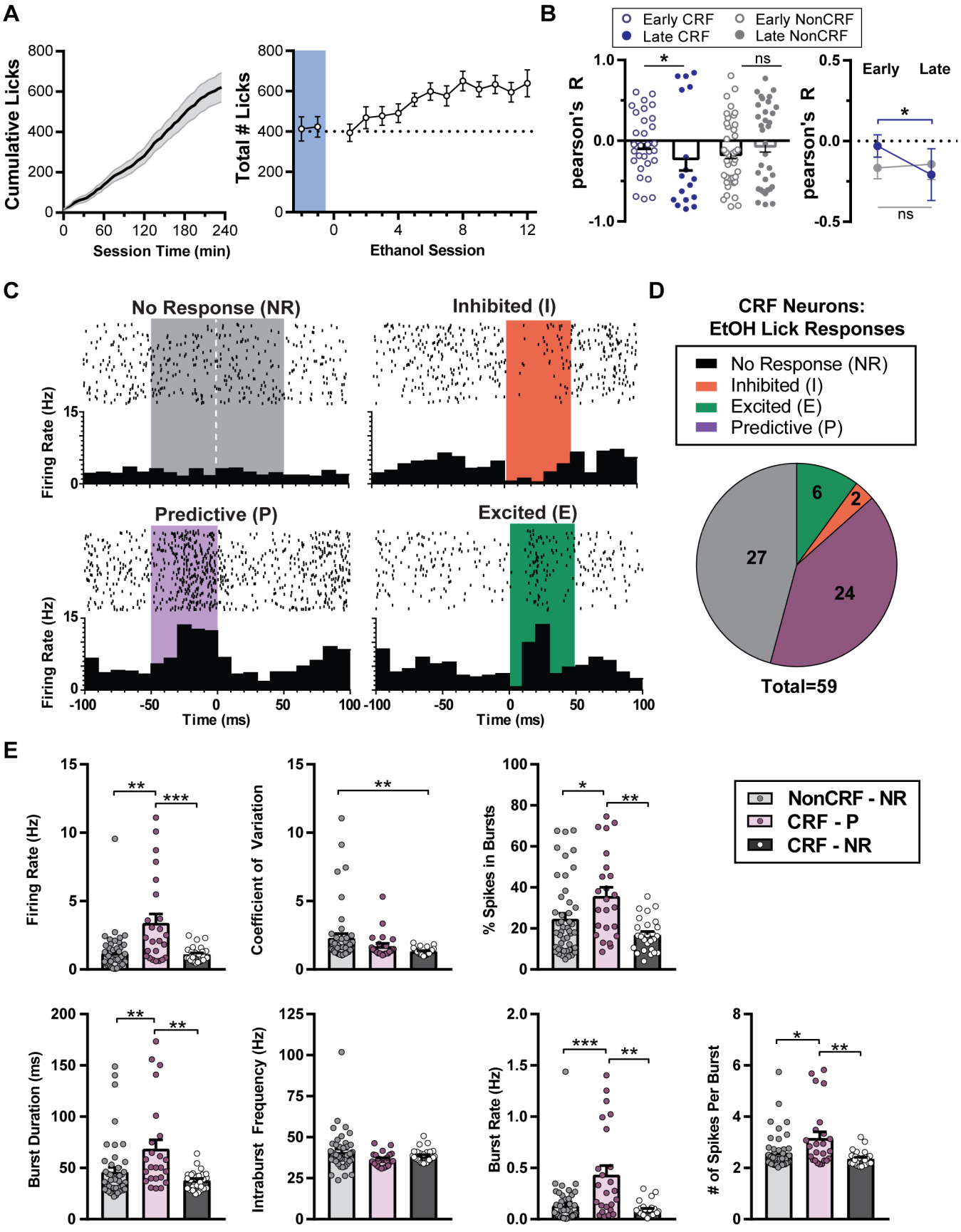

Irving, Aroni, and Sparta 2018

Figure 3.

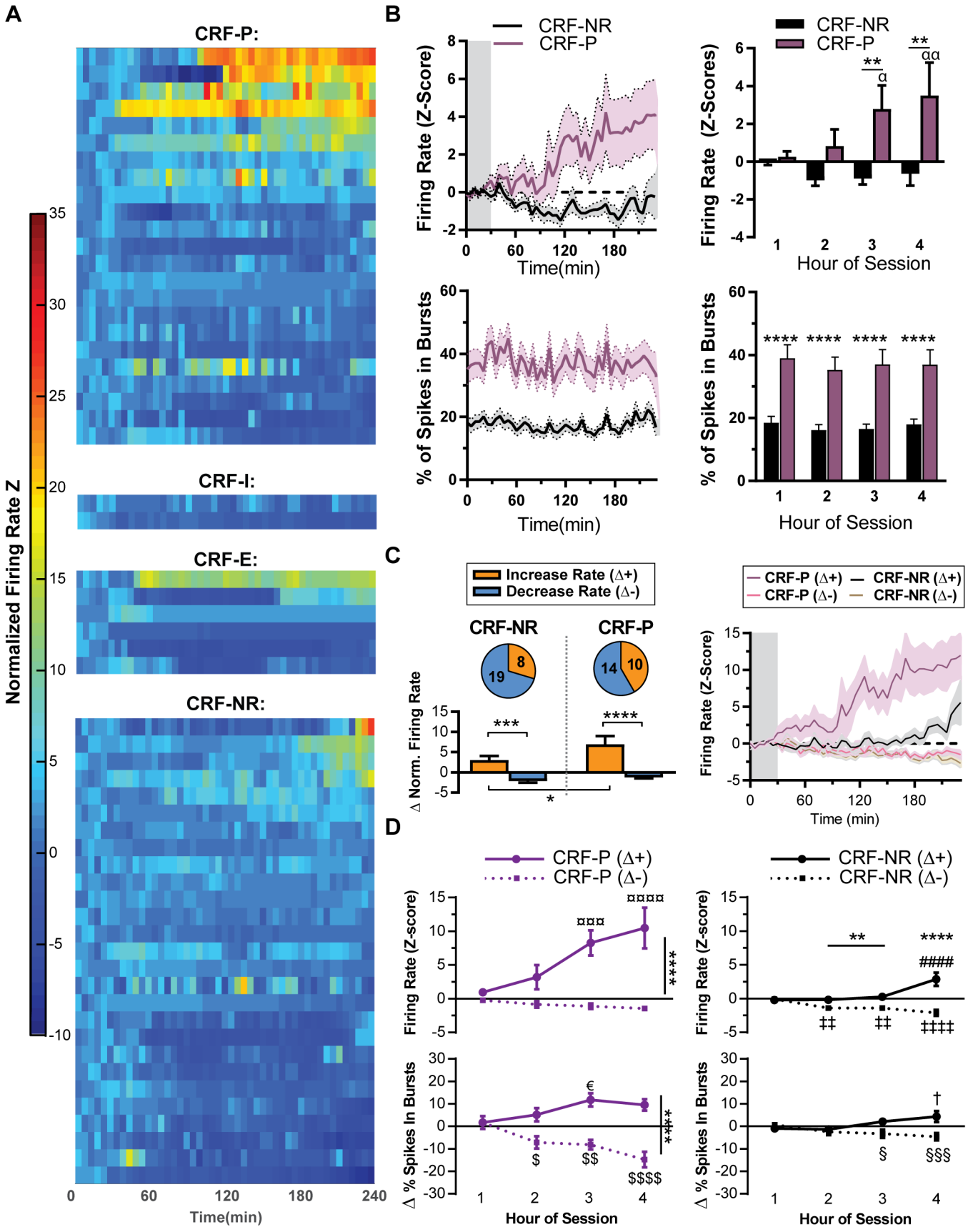

Irving, Aroni, and Sparta 2018

Figure 4